Available online at www.sciencedirect.com
SCIENCE DIRECT®
Polymer 45 (2004) 2843–2852
polymer
www.elsevier.com/locate/polymer

Structural analysis of cellulose triacetate polymorphs by two-dimensional solid-state $^{13}C-^{13}C$ and $^{1}H-^{13}C$ correlation NMR spectroscopies

Hiroyuki Kono[a,*], Yukari Numata[b], Tomoki Erata[b,1], Mitsuo Takai[b]

[a]*Bruker BioSpin Company Ltd, Tsukuba, Ibaraki 305-0051, Japan*
[b]*Division of Molecular Chemistry, Graduate School of Engineering, Hokkaido University, Sapporo, Hokkaido 060-8628, Japan*

Received 10 October 2003; received in revised form 15 January 2004; accepted 31 January 2004

Abstract

For the elucidation of the crystal structures of the two crystalline allomorphs of cellulose triacetate (CTA), namely CTA I and CTA II, two-dimensional (2D) solid-state through-bond $^{13}C-^{13}C$ and $^{1}H-^{13}C$ correlations NMR techniques applied to the two crystalline allomorphs of CTA. As a result, the ^{13}C and ^{1}H chemical shifts of the glucopyranose ring of CTA I and CTA II were completely assigned by the 2D NMR spectra of these allomorphs. On the 2D $^{13}C-^{13}C$ correlation spectrum of CTA II, two sets of the $^{13}C-^{13}C$ correlations from C1 to C6 were observed. This indicated that the CP/MAS ^{13}C NMR spectrum of CTA II can be characterized by its overlapping of the ^{13}C subspectra of two kinds of 2,3,6-triacetyl-anhydroglucopyranose units and that there are two magnetically non-equivalent sites in the unit cell of CTA II. In the case of CTA I, the numbers of respective ^{13}C and ^{1}H shifts of CTA I agreed with the those of the glucopyranose residue in the allomorph, strongly suggesting that the asymmetric unit of CTA I is only one glucose residue. In addition, conformational differences in the exocyclic C5–C6 bonds between CTA I and CTA II were strongly suggested by the notable differences in the ^{1}H and ^{13}C chemical shifts at the C6 sites of these allomorphs.

Keywords: Cellulose triacetate; 2D Solid-state NMR; Polymorphs

1. Introduction

Cellulose triacetate (CTA) has two crystalline allomorphs, CTA I and CTA II. As shown in Scheme 1, Sprague et al. [1] in 1958 established a clear relationship between various preparative schemes for CTA and the two allomorphs. According to this scheme, CTA I is produced only by heterogeneous acetylation from cellulose I, while CTA II is obtained from heterogeneous acetylation of cellulose II and homogeneous acetylation of cellulose followed by the crystallization of the formed CTA. Sprague et al. also demonstrated that the saponification of CTA I and CTA II provides the corresponding polymorphs of cellulose [1]. This suggested that the chain polarity was preserved in going from cellulose I and CTA I or cellulose II to CTA II.

A number of reports on the crystal structures of CTA allomorphs have been based on fiber diffraction patterns to elucidate the chain polarities of CTA I [2] and CTA II [3,4]. Among the proposed structures of the CTAs, the parallel packing model [2] for CTA I and the antiparallel model [3] CTA II have been generally accepted. For CTA I, Stipanovic and Sarko [2] proposed that the structure packs in two parallel chains, which together form an orthorhombic unit cell with $P2_1$ symmetry; this proposal was based on a combination of X-ray fiber diffraction patterns and stereochemical model analysis. In the case of CTA II, Roche et al. [3] proposed the antiparallel arrangement model based on fiber patterns. The unit cell of CTA II contains four chains: two parallel and two antiparallel. The two chains in each parallel pair and in each antiparallel pair are related via 2_1 screw axes positioned outside of the chains. In addition, discussions that link chain polarities in CTA I and CTA II to chain polarities in cellulose I and cellulose II, respectively, have been offered by many researchers. Fiber patterns of X-ray, electron, and neutron diffractions supported that the chains are parallel in cellulose I [5–7] and antiparallel in cellulose II [8–10]. It has therefore, been considered that

* Corresponding author. Tel.: +81-29-852-1235; fax: +81-29-858-0322.
E-mail addresses: hiroyuki.kono@bruker-biospin.jp (H. Kono), erata@dove-mc.eng.hokudai.ac.jp (T. Erata).
[1] Tel./fax: +81-11-706-6566.

0032-3861/$ - see front matter © 2004 Elsevier Ltd. All rights reserved.
doi:10.1016/j.polymer.2004.01.075

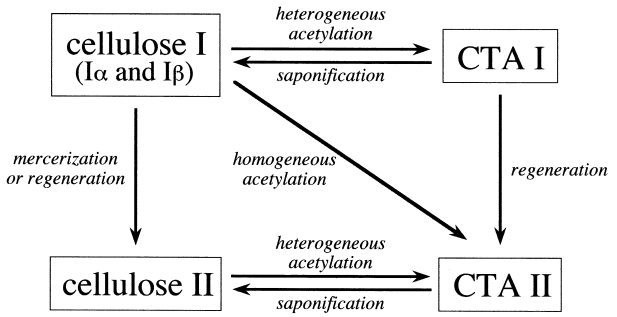

Scheme 1. Relationships between cellulose and cellulose triacetate allomorphs.

the chains are parallel in cellulose I and CTA I and antiparallel in cellulose II and CTA II.

On the other hand, other researchers have reported experimental results that conflict with the strong relationship Sprague proposed. For example, CTA I was produced from heterogeneous acetylation of cellulose II pretreated with glacial acetic acid [11,12]. In addition, it was reported that CTA I produced from heterogeneous acetylation of cotton cellulose was transformed into CTA II in the presence of formic acid, and that this CTA II saponified into cellulose I, in contrast to Sprague's scheme [13]. VanderHart et al. [14] demonstrated that CTA oligomers prepared from homogeneous acetylation of the cellodextrins crystallized into a CTA I lattice by the Raman and CP/MAS ^{13}C NMR spectroscopic analyses, which was supported by other researchers based on the X-ray diffraction observations of the CTA oligomers [15]. Therefore, the discussions regarding the structures of the allomorphs of the CTAs as well as those of cellulose are in progress, including the main topic of chain polarity of the cellulose and CTA polymorphs.

A structural analysis of the CTAs by employing solid-state ^{13}C NMR has already been published. Through ^{13}C NMR spectroscopic analysis, Horii et al. [16] demonstrated that CTA I returns to cellulose I_β by the saponification treatment. VanderHart et al. [14] isolated the spectra of the CTA I and CTA II lattices and non-crystalline CTA from the CP/MAS ^{13}C NMR spectra of various preparations of CTAs. After splitting the ^{13}C signals of crystalline CTA allomorphs, those authors revealed that CTA I has only one magnetic environment in the unit cell, whereas the unit cell of CTA II has at least two magnetically non-equivalent sites. In addition, Raman observations led them to conclude that CTA I and CTA II are distinguished by differences in the backbone conformation. Very recently, we reported the complete assignment of ^{13}C resonance lines of the ring carbon of CTA I and that of CTA II by using ^{13}C-enriched CTAs site-specifically [17]. The ^{13}C-enriched samples were prepared from ^{13}C-enriched bacterial celluloses that had been biosynthesized from D-(2-^{13}C), D-(3-^{13}C), or D-(5-^{13}C)glucose. As a result, it was revealed that all carbons of CTA I appeared as singlets, while those of CTA II except for C1 are shown as equal-intensity doublets in the ^{13}C spectrum of this allomorph. Based on the notable difference in the C6 chemical shifts of CTA I and CTA II, we suggested that CTA I and CTA II were distinguished by the conformational differences in C5–C6 exocyclic bonds.

The present study demonstrates the two-dimensional (2D) through-bond ^{13}C homonuclear correlation spectrum of CTA II by using a refocused CP-INADEQUATE experiment [18] in order to derive the ^{13}C subspectra of anhydroglucose residues contained in the unit cell of CTA II. In addition, ^{1}H chemical shifts of the protons attached directly to ring carbons of CTA I and CTA II are assigned from the 2D through-bonds ^{13}C–^{1}H correlation [19,20] spectra of these allomorphs for the first time. From the ^{13}C and ^{1}H chemical shifts of CTA I and CTA II, conformational differences between these allomorphs are also discussed.

2. Experimental

2.1. Specimens

^{13}C-Enriched cellulose was biosynthesized by *Acetobacter xylinum* (*A. xylinum*) ATCC10245 from Hestrin and Schramm medium [21] containing 1% (v/v) of ethanol and 3% each of D-(1-^{13}C), D-(2-^{13}C), D-(3-^{13}C), D-(4-^{13}C), D-(5-^{13}C), and D-(6-^{13}C)glucoses (Cambridge Isotope Laboratories, Inc., MA; the isotropic purity of all labeling compounds was 99%) in unlabeled glucose. Biosynthesis was carried out at 28 °C for 7 days under static conditions. The bacterial cellulose was purified according to the method described previously [17,22]. CTA I was prepared from ramie cellulose by heterogeneous acetylation using the method of Tanghe et al. [23] CTA II was prepared from ramie or ^{13}C-enriched bacterial cellulose according to the method described previously [22]. The crystallinity of the CTA samples was improved by heat treatment at 220 °C for 15 min under nitrogen [14,17,24] and then confirmed by X-ray diffraction before the solid-state NMR experiments. The X-ray diffractograms were measured on a Rigaku Rint-2000 diffractometer by refraction method using nickel-filtered Cu K_α radiation operated in ω–2θ scanning mode between 5 and 30° (2θ) [15,17]. Slit system were 1° for divergence, 0.15 mm for receiving, and 1° for scatter. The degree of substitution of each sample was determined according to the usual titration method [25].

2.2. Solid-state NMR experiments

All NMR experiments were carried out on a Bruker AV 300 wide-bore spectrometer (Bruker BioSpin Co. Ltd, Karlsruhe, Germany; proton frequency, 300.13 MHz) at room temperature. The pulse sequences for the experiments used in this study are shown in Fig. 1. CP/MAS ^{13}C NMR (Fig. 1(A)) spectra of CTA samples were obtained using a Bruker BL4 4-mm double-tuned MAS probe. The sample

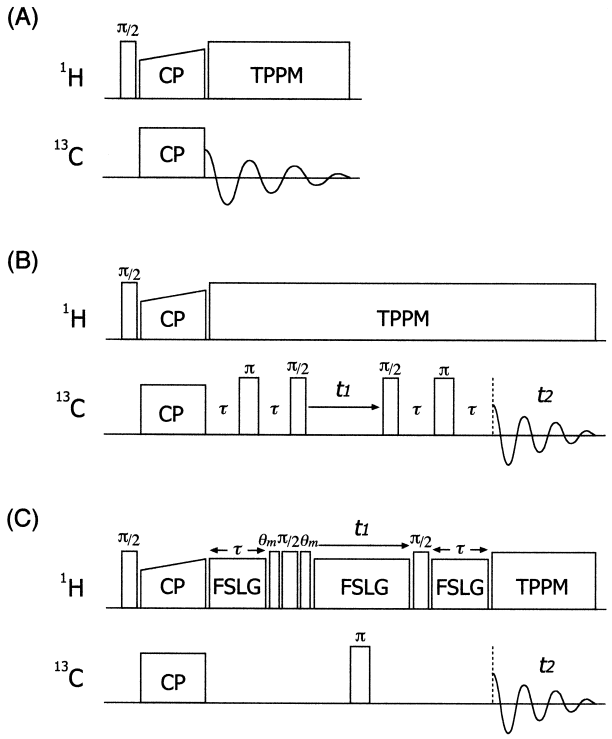

Fig. 1. Pulse sequences for the CP/MAS ^{13}C NMR (A), 2D refocused INADEQUATE (B) and 2D MAS-J-HMQC (C) experiments. The phase cycle for the INADEQUATE and that for MAS-J-HMQC were adapted from Refs. [18,19], respectively. θ_m is a magic angle (54.7°) pulse.

volume was about 80 μl and the MAS frequency was set to 12 kHz. For the cross-polarization step, the radio frequency field strength was set to 70 kHz for carbon, while a ramped radio frequency field (RAMP-CP) [26] was applied on the proton and matched to optimize the ^{13}C signal resolution of the carbonyl carbon resonance of D-glycine. During the acquisition period, TPPM proton decoupling [27] was applied with a proton field strength of 72 kHz. The contact time and the repetition time were set to 1 ms and 4 s, respectively. The refocused CP-INADEQUATE experiment (Fig. 1(B)) was performed according to the method of Lesage et al. [18] with several modifications, using a Bruker BL7 7-mm double-tuned MAS probe. The sample volume was about 280 μl and the MAS frequency was set to 6 kHz. For the cross-polarization step, a RAMP-CP was applied to the proton field strength and the contact time was set to 1 ms. During the acquisition period, TPPM proton decoupling was applied to a proton field strength of 72 kHz. The 180° pulse on carbons was set to 7.6 μs. Using the TPPM scheme, the proton decoupling field strength was 72 kHz. The repetition time was set to 2 s. The quadrature was detected using the TPPI method [28]. A total of 128 t_1 increments, with 1024 scans per increment, was collected. The MAS-J-HMQC experiment (Fig. 1(C)) was measured using a Bruker BL4 4-mm double-tuned MAS probe according to the method of Lesage et al. [19,20]. The sample volume was restricted to 25 μl and set to the center of the sample rotor to improve the homogeneity of the radiofrequency field. The MAS frequency was set to 12 kHz. The proton radiofrequency field strength was set to 72 kHz during acquisition using the TPPM scheme and to 81 kHz during the frequency-switched Lee-Goldberg (FSLG) [29,30] decoupling. The delay for FSLG time was set to 3.1 ms, and two off-resonance pulses with opposite phases in the FSLG decoupling were set to 8.8 μs. The magic angle pulse length, CP time, and repetition time were set to 2.0 μs, 800 μs, and 2 s, respectively. The quadrature was detected using the States method [31]. A total of 96 t_1 increments, with 1024 scans per increment, was collected. In all NMR experiments, the ^{13}C chemical shifts were calibrated through the carbonyl carbon resonance of D-glycine as an external reference at 176.03 ppm. In the refocused INADEQUATE experiments, the double quantum frequency (DQ) scale (vertical axis) was calibrated by use of an L-alanine mixture prepared by dissolving and recrystallizing 20% fully ^{13}C enriched L-($^{13}C_3$)alanine together with 80% non-enriched L-alanine. Since the assignments for the alanine ^{13}C spectrum are CH_3 (20.2 ppm); CH (50.7 ppm) and COOH (178.1 ppm), DQ of correlation between CH_3 and CH and that between CH and COOH in the INADEQUATE spectrum of the alanine mixture were set to 70.9 and 228.8 ppm, respectively. In the MAS-J-HMQC spectra, the proton chemical shift scale was collected for the scaling factor of $1/\sqrt{3}$ (in theory, a ^{1}H chemical shift is scaled by $1/\sqrt{3}$ under FSLG decoupling) [29,30]. The ^{1}H chemical shifts of the protons attached to carbon nuclei were determined by estimating the highest peak of the proton trace extracted in the ^{1}H direction from the MAS-J-HMQC spectrum.

3. Results and discussion

3.1. 2D ^{13}C–^{13}C correlation spectrum of CTA II

The CTA I and CTA II samples were prepared by heterogeneous acetylation and by solution acetylation of cellulose, respectively. The CTAs were subsequently exposed to sufficient thermal treatment at 220 °C for 15 min (the glass transition temperature of CTA is 175–189 °C [12,14]) to enhance their crystallinities. The crystallinities and allomorphs of the samples were confirmed by X-ray diffraction before the CP/MAS ^{13}C NMR measurements [15,17]. Fig. 2(A) and (B) shows the CP/MAS ^{13}C NMR spectra of CTA I and CTA II, respectively, both derived from ramie cellulose. According to the previous report [14] on the CTA, crystalline and non-crystalline components can be easily distinguished by the ^{13}C spectral lineshape, especially the carbonyl and methyl carbons region. In the carbonyl carbon region, there are a doublet and a quintet splitting for CTA I and CTA II, respectively. In the case of methyl carbon, the sharper doublet for CTA I with a 1 ppm splitting was observed, and CTA II spectrum has a wider doublet (ca. 2.5 ppm) whose downfield peak has

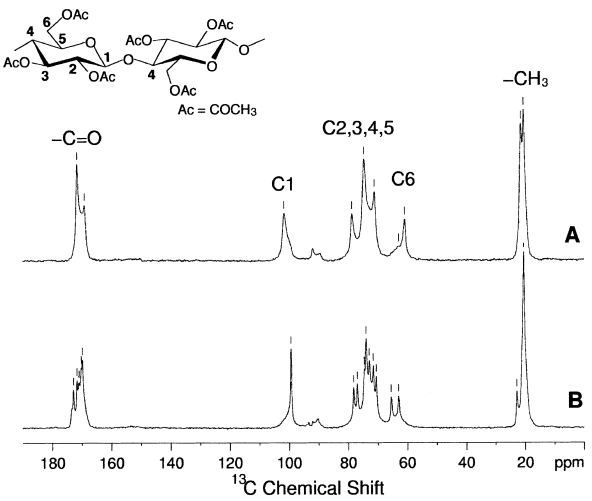

Fig. 2. 1D CP/MAS ^{13}C NMR spectra of CTA I (A) and CTA II (B) obtained from ramie cellulose.

much less intensity in comparison with that of CTA I. On the other hand, non-crystalline CTA shows a respective singlet with broad linewidth in the both methyl and carbonyl carbon regions. As can be seen in Fig. 2(A) and (B), these samples show general features of the ^{13}C spectra of highly crystallized CTA I and CTA II, respectively.

In the spectra of CTA I and CTA II, the notable difference between these allomorphs was observed in the ring carbon region of these spectra; CTA I exhibits a resonance for C1 at 102 ppm and CTA II possesses one at 99 ppm. The resonances at C6 are distinctive, with a singlet appearing at 61 ppm for CTA I and a doublet displayed by CTA II at 66 and 63 ppm. On the other hand, the C2–C5 resonances of both allomorphs had not been assigned for a long time since a number of resonance lines overlapped in the narrow region (80–68 ppm) of the ^{13}C spectra, in contrast to the relatively simple ^{13}C resonance lines for C1 and C6. Very recently, the C2–C5 signals of both CTA allomorphs were assigned by the lineshape analysis of the CP/MAS ^{13}C spectra of site-specifically ^{13}C-enriched CTA samples [17]. The results of the assignment are shown in Fig. 3, which is a magnification of the ring carbon region of the CTA spectra (Fig. 2). The ^{13}C chemical shift data are summarized in Table 1. According to the assignment, each ring carbon of CTA I appeared as a singlet, although the C2 and C3 signals overlapped at 75 ppm in the ^{13}C spectrum of this allomorph. In the case of CTA II, all carbons appeared as equal-intensity doublets except for C1, suggesting that CTA II has two kinds of anhydroglucose units in the unit cell [17]. However, the full exploitation of the CP/MAS ^{13}C NMR spectrum of CTA II is far from complete since the ^{13}C signals of each glucopyranose residue composing the structure of CTA II have not been identified. Therefore, the 2D through-bonds $^{13}C-^{13}C$ correlation spectrum of CTA II was measured for the detailed interpretation of the CP/MAS ^{13}C spectrum of CTA II.

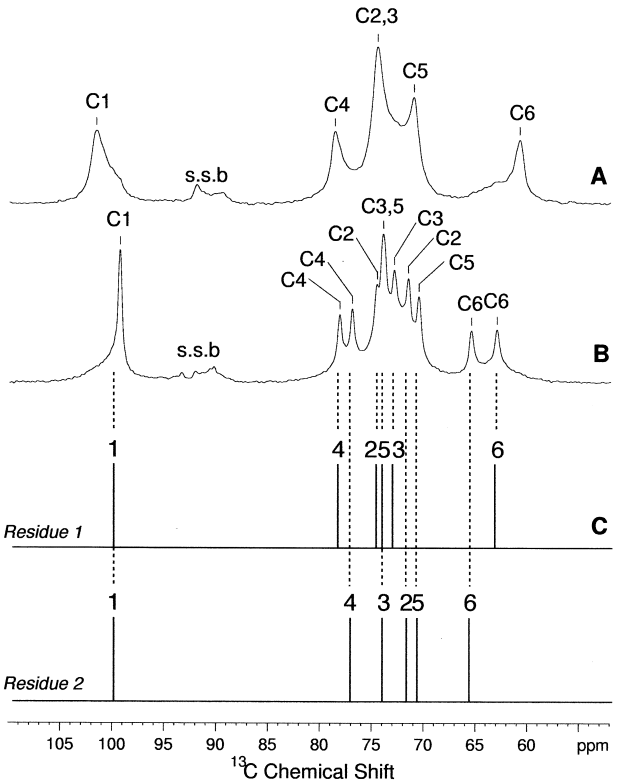

Fig. 3. Expanded 1D CP/MAS ^{13}C NMR spectra for ring carbon region of CTA I (A) and CTA II (B) obtained from ramie cellulose. The abbreviation 's.s.b.' indicates spinning side band. ^{13}C Line spectra of the two magnetically non-equivalent anhydroglucose residues composing CTA II (C). The lines indicate the ^{13}C chemical shifts of each carbon of the anhydroglucose residues. The line spectra were determined by the INADEQUATE spectrum of the ^{13}C-enriched CTA II (Fig. 5).

Since the natural abundance of ^{13}C nuclei is ca. 1.1%, it is difficult to obtain the $^{13}C-^{13}C$ correlation peaks of naturally abundant compounds in multi-dimensional experiments of solid-state NMR. In this study, therefore, we prepared the ^{13}C-enriched CTA II from bacterial cellulose biosynthesized from 3% each of D-(1-^{13}C), D-(2-^{13}C), D-(3-^{13}C), D-(4-^{13}C), D-(5-^{13}C), and D-(6-^{13}C) glucoses, and the crystallinity of the ^{13}C-enriched CTA II was improved by the heat-treatments at 220 °C. Fig. 4(A) and (B) shows the CP/MAS ^{13}C spectra of the ^{13}C-enriched CTA II and non-labeled CTA II prepared from ramie cellulose, respectively. The ^{13}C-enriched CTA II showed highly crystallized CTA II patterns and spectral characteristics similar to those of CTA II prepared from ramie cellulose, except for the increase in the ^{13}C signal intensity of ring carbons. This finding indicated that the ^{13}C-enriched CTA II was highly crystallized CTA II, of which only the ring carbons were selectively ^{13}C-enriched. Fig. 5 shows the ring carbon region of the refocused CP-INADEQUATE spectrum of the ^{13}C-enriched CTA II. In the 2D spectrum, as previously described by Lesage et al. [18], two directly bonded carbons share a common frequency in the DQ dimension and the ^{13}C chemical shift of each carbon corresponds to a frequency in the single quantum dimension. In the spectrum,

Table 1
^{13}C and ^{1}H resonance assignments of CTA I and CTA II

Allomorph		^{13}C Chemical shifts/ppm (^{1}H chemical shifts/ppm)					
		C1 (H1)	C2 (H2)	C3 (H3)	C4 (H4)	C5 (H5)	C6 (H6)
CTA I	Ref. [17][a]	102.4	76.2	76.2	80.3	72.9	62.5
		101.6 (4.1)	74.5 (3.5)	74.5 (3.5)	78.6 (2.2)	71.0 (2.9)	60.8 (2.3)
CTA II	Ref. [17][a]	100.4	76.6, 73.5	75.8, 74.8	80.1, 78.7	75.8, 72.5	67.3, 65.2
	Residue 1 (solid line)[b]	99.4 (4.3)	74.6 (3.8)	72.9 (4.1)	78.2 (2.4)	73.9 (4.5 or 3.4[c])	63.0 (2.3)
	Residue 2 (dotted line)[b]	99.4 (4.3)	71.5 (3.7)	73.9 (4.5 or 3.4[c])	76.9 (2.4)	70.5 (3.4)	65.5 (2.3)

[a] Chemical shift data for CTA I and CTA II in Ref. [17] differ from those in this study by ca. 1.5 ppm.
[b] Two kinds of the 2,3,6-triacetyl-anhydroglucose residues in the structure of CTA II, which was revealed by the 2D refocused INADEQUATE spectrum of ^{13}C-enriched CTA II (Fig. 5). Through-bond $^{13}C-^{13}C$ connectivities of the carbons in the residues 1 and 2 were shown by the solid and dotted lines in the 2D spectra, respectively.
[c] ^{1}H chemical shift of the proton attached to C5 in the residue 1 and that attached to C3 of the residue 2 could not determined by the MAS-J-HMQC spectrum of CTA II (Fig. 8) because ^{13}C resonance lines for these carbons overlap in the spectrum.

the C1 signal of CTA II appearing at 99 ppm was separated into two cross-peaks in the DQ dimension; one appeared at 174 ppm in the DQ frequency, while the other appeared at 170 ppm. Therefore, it is possible to sequentially assign each ^{13}C resonance of the glucopyranose ring in CTA II in a relatively straightforward manner by using the refocused INADEQUATE spectrum and starting from the two anomeric C1 signals. As indicated by the solid lines in this figure, the C2 resonance can be identified at 75 ppm since this is the only resonance correlated with C1 resonance at 170 ppm of DQ frequency. The C2 has a second clear correlation in the DQ dimension at 147 ppm, leading to the identification of C3 at 73 ppm. In addition, the C3 at 73 ppm also correlates with C4 at 78 ppm in the DQ dimension at 151 ppm, and the C4 has a second correlation with C5 at 74 ppm in the DQ dimension at 152 ppm. Finally, the ^{13}C signal at 63 ppm can be assigned as C6, which binds to C5 appearing at 74 ppm, since the carbons share a common DQ frequency of 137 ppm. In addition, as indicated by the dotted lines in this spectrum, the remaining ^{13}C resonance lines for C1 through C6 of CTA II can be connected, starting from the C1 signal in the DQ frequency of 170 ppm. These findings indicated that chemical shifts of all carbons composing two kinds of glucopyranose residues in the unit cell of CTA II could be assigned by the refocused INADEQUATE spectrum of the ^{13}C-enriched CTA II. The ^{13}C chemical shifts of the two kinds of glucopyranose residues in CTA II are illustrated by the lines in Fig. 3(C), and the shift data are summarized in Table 1.

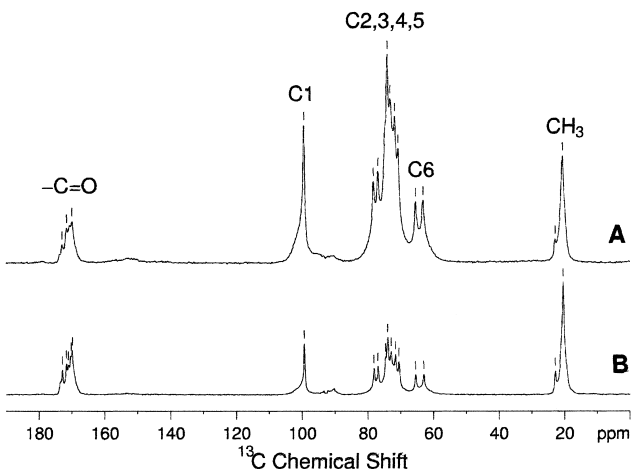

Fig. 4. 1D CP/MAS ^{13}C NMR spectra of CTA II prepared from ramie cellulose (A) and ^{13}C-enriched bacterial cellulose (B). The ^{13}C-enriched bacterial cellulose was biosynthesized by *A. xylinum* ATCC10245 from the mixture of D-(1-^{13}C), D-(2-^{13}C), D-(3-^{13}C), D-(4-^{13}C), D-(5-^{13}C), and D-(6-^{13}C) glucoses.

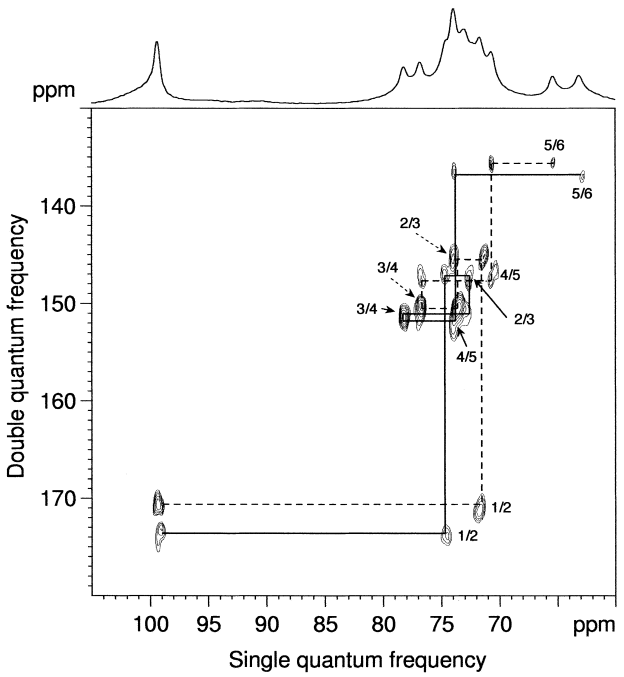

Fig. 5. Expanded 2D refocused INADEQUATE spectrum for ring carbon region of CTA II biosynthesized by *A. xylinum* ATCC10245 from the mixture of D-(1-^{13}C), D-(2-^{13}C), D-(3-^{13}C), D-(4-^{13}C), D-(5-^{13}C), and D-(6-^{13}C) glucoses.. 1D CP/MAS ^{13}C NMR spectrum of the ^{13}C-enriched CTA II is shown above the 2D spectrum. The solid and dotted lines in the 2D spectrum indicate through-bond $^{13}C-^{13}C$ connectivities of two kinds of glucopyranose residues composing of CTA II.

3.2. 2D $^{1}H-^{13}C$ heteronuclear correlation spectra of CTA I and CTA II

Next, the 2D MAS-J-HMQC spectra of both CTA I and CTA II were measured by using CTA samples prepared from ramie cellulose to assign the ^{1}H chemical shifts of the protons bonded to each carbon atom of both allomorphs. Fig. 6(A) and (B) shows the expansion of the methyl carbon regions of the MAS-J-HMQC spectra CTA I and CTA II, respectively. This experiment provided an isotropic chemical shift correlation between pairs of directly bonded carbon and proton nuclei [20,32]. Therefore, the methyl carbons of both allomorphs were correlated with their attached protons, whereas the carbonyl carbons give no cross-peaks in the column direction (data not shown). In the methyl carbon region of the CP/MAS ^{13}C spectrum of CTA I, a sharper doublet with a 1.0 ppm splitting was observed. On the other hand, methyl resonances of CTA II appear as a multiplet, and some shoulders were observed in the upfield peak in the region of 22–18 ppm. The methyl carbon region of the 2D $^{1}H-^{13}C$ correlation spectra of CTA I and CTA II provided a new finding that suggests the structural difference between these allomorphs. In the case of CTA I, the carbon doublet appearing at 21.2 and 20.1 ppm provided the respective cross-peaks at the ^{1}H chemical shift of 0.8 ppm. For the methyl carbon of CTA II, the downfield resonance at 22.7 ppm gave a $^{1}H-^{13}C$ cross-peak in the ^{1}H chemical shifts of 1.7 ppm, while the upfield peak appearing at 22–18 ppm provided a complex $^{1}H-^{13}C$ multiplet pattern. The multiplet contains at least three $^{1}H-^{13}C$ cross-peaks whose ^{13}C chemical shifts were 20.8, 20.2, and 19.5 ppm. The ^{1}H chemical shifts of protons attached to these methyl carbons appearing at 20.8, 20.2, and 19.5 ppm are 1.1, 0.6, and 1.1 ppm, respectively. In addition to these three correlations, some tailings could be observed in the multiplet along with the ^{1}H chemical shift axis, indicating that some $^{1}H-^{13}C$ correlations are contained in the multiplet pattern besides the three correlations at 20.8, 20.2, and 19.5 ppm. The ^{1}H and ^{13}C chemical shift data of the methyl groups of CTA I and CTA II are summarized in Table 2, with the ^{13}C chemical shifts of carbonyl carbons of these allomorphs.

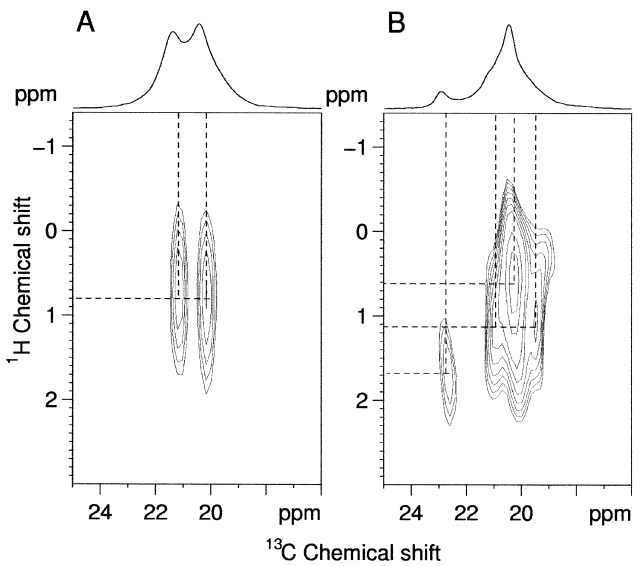

Fig. 6. Expanded 2D MAS-J-HMQC spectra for methyl carbon region of CTA I (A) and CTA II (B) obtained from ramie cellulose. 1D CP/MAS ^{13}C NMR spectra of the CTA samples are shown above the 2D spectra.

Figs. 7 and 8 display the ring carbon region of the MAS-J-HMQC spectra of CTA I and CTA II, respectively. Since the ^{13}C signals of CTA I and CTA II in this region were completely assigned, the isotropic ^{1}H chemical shift of protons attached to the ring carbons of both allomorphs could be assigned by the $^{1}H-^{13}C$ correlation spectra. In the MAS-J-HMQC spectrum of CTA I, ^{1}H chemical shifts of the protons attached to C1, C4, and C5 could be assigned as 4.1, 2.2, and 2.9 ppm, respectively, because these carbons provided the $^{1}H-^{13}C$ cross-peaks at these positions. A singlet of C6 resonance provided unresolved two cross-peaks at the ^{1}H chemical shift of 2.3 and 3.7 ppm. However, the lower cross-peak at 3.7 ppm should be some noise because the intensity is too low and the line width along the ^{13}C chemical shit axis is also too narrow, indicating that two protons attached to C6 have the same chemical shift of 2.3 ppm. The remaining C2 and C3 resonances, which overlapped at 75 ppm in the CP/MAS ^{13}C spectrum, provided $^{1}H-^{13}C$ cross-peaks at 3.5 ppm of the ^{1}H chemical shift. Since the cross-peaks correlated with C2 and C3 resonances overlapped each other, the ^{1}H resonance lines of the protons attached to C2 and C3 had the same chemical shift, 3.5 ppm. The ^{1}H chemical shifts of the protons of CTA I are summarized in Table 1.

In the case of CTA II, as shown in Fig. 8, since the structure of this allomorph contains two kinds of glucopyranose

Table 2
^{13}C and ^{1}H chemical shifts of acetyl groups in CTA I and CTA II

Allomorph	^{13}C Chemical shifts/ppm (^{1}H shifts/ppm)	
	C=O[a]	CH_3[b]
CTA I	171.4	21.2 (0.8)
	169.1	20.1 (0.8)
CTA II	172.9	22.7 (1.7)
	171.7	20.8 (1.1)[c]
	171.0	20.2 (0.6)[c]
	169.9	19.5 (1.1)[c]
	169.6	

[a] ^{13}C Chemical shift data for carbonyl carbons of CTA I and CTA II were assigned from the 1D CP/MAS ^{13}C spectra of these allomorphs (Fig. 2).
[b] ^{13}C and ^{1}H chemical shifts of the methyl groups of CTA I and CTA II were assigned from the MAS-J-HMQC spectrum of these allomorphs (Fig. 6).
[c] In addition to three $^{1}H-^{13}C$ correlations for methyl carbons of CTA II, some tailings were observed in Fig. 5(B).

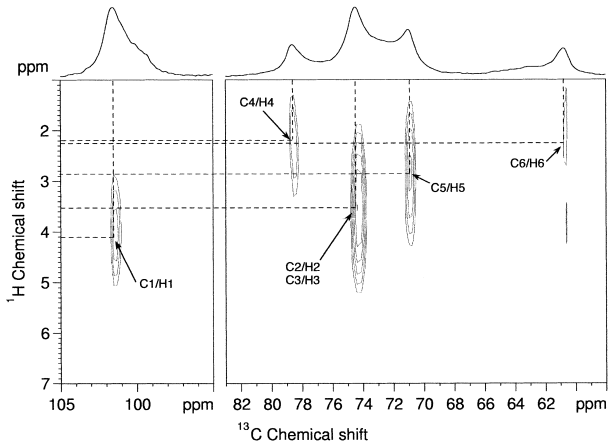

Fig. 7. Ring carbon region of the MAS-J-HMQC spectrum of CTA I prepared by the acetylation of ramie cellulose. The 1D CP/MAS ^{13}C NMR spectrum of the CTA I is shown above the 2D spectrum.

residues in the unit cell, a number of ^{1}H–^{13}C cross-peaks could be observed in the spectrum in comparison with the number of cross-peaks in the CTA I spectrum. The singlet at 99 ppm, composed of the overlap of two kinds of C1 signals of CTA II, gave only one cross-peak at the ^{1}H chemical shifts of 4.3 ppm. Since the line width of the ^{1}H resonance in the C1 cross-section was narrower than or equal to those in the other carbon cross-sections (data not shown), each proton attached to C1 of two kinds of glucopyranose residues in CTA II had the same ^{1}H chemical shift of 4.3 ppm. For the other carbons, each carbon resonance provided a ^{13}C–^{1}H correlation peak, leading to the assignment of the ^{1}H chemical shifts of protons directly bonded to the carbon nuclei. For example, the ^{1}H chemical shift of a proton attached to C4 whose ^{13}C signal appears at 78 ppm could be assigned to 2.4 ppm, since the cross-peak correlated with the C4 resonance appeared at 2.4 ppm in the ^{1}H dimension. Using a similar method, the ^{1}H chemical shifts of proton attached to the C4 enabled the assignment of ^{1}H shifts of the protons, as summarized in Table 1. With respect to the protons at C6 sites, since each C6 carbon binds to two protons, each ^{13}C signal of the C6 doublet appearing at 64.8 and 62.3 ppm should correlate with two ^{1}H–^{13}C cross-peaks. However, both C6 resonances correlated with the respective one cross-peak at 2.3 ppm of the ^{1}H shift, indicating that the ^{1}H chemical shifts of four protons attached to two kinds of C6 were all at 2.3 ppm. In the MAS-J-HMQC spectrum of CTA II, the ^{1}H–^{13}C correlation peaks have different intensities for C4 and C6 doublets. The efficiency of carbon signal intensity depends on the ^{13}C linewidth and the heteronuclear scalar J_{CH} coupling [19]. The delay for FSLG time (τ delay in Fig. 1(C)) was set to 3.1 ms for the MAS-J-HMQC experiment. If another τ delay were used, the intensity of correlations for C4 and C6 might become stronger while the other correlations would become weaker.

In general, ^{1}H resonances of solids with high proton density such as CTA are considerably broadened by strong ^{1}H–^{1}H homonuclear dipolar interactions. In this experiment, a relatively high MAS frequency of 12 kHz was used for the sample rotation in order to suppress the strong ^{1}H homonuclear dipolar interaction and to enhance ^{1}H resolution. In addition, the sample volume was restricted to about 25 μl and set to the center of the sample rotor for the enhancement of the radiofrequency field homogeneity. If these ^{1}H–^{13}C correlation experiments of CTA samples could be performed by use of the NMR instrument with higher magnetic field strength and higher MAS frequency of sample rotation, ^{1}H–^{13}C correlation peaks associated with C6 carbons of CTA I and CTA II might be split into two.

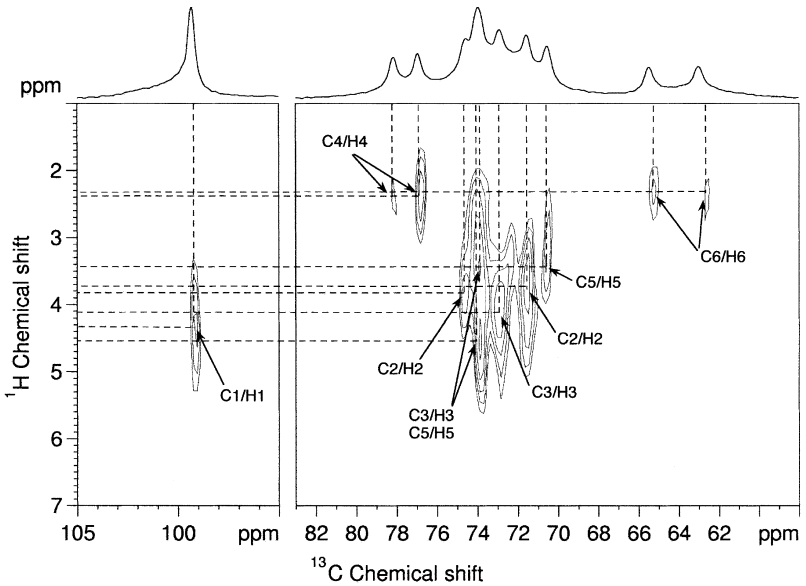

Fig. 8. Ring carbon region of the MAS-J-HMQC spectrum of CTA II prepared by the acetylation of ramie cellulose. The 1D CP/MAS ^{13}C NMR spectrum of the CTA II is shown above the 2D spectrum.

3.3. Structures of CTA I and CTA II

This study provided the ^{13}C and ^{1}H chemical shifts of the glucopyranose residues contained in the unit cells of CTA I and CTA II by use of the through-bond $^{13}C-^{13}C$ and $^{1}H-^{13}C$ correlation spectra of these crystalline allomorphs. As summarized in Table 1, the ^{13}C chemical shift data of the ring carbons of CTA II, which were assigned by the refocused INADEQUATE experiment, agreed with those estimated by the lineshape analysis of CP/MAS ^{13}C NMR spectra of the site-specifically ^{13}C-enriched CTA samples [17]. In addition, it was directly proven by the through-bond $^{13}C-^{13}C$ correlation spectra of CTA II that there are two kinds of glucopyranose residues in the unit cell of this allomorph (Fig. 5), which agreed with previous suggestions [17]. In a previous report [17], the lineshape analysis of the CP/MAS ^{13}C spectrum of highly crystalline CTA II revealed that all carbons of CTA II except for C1 appeared as equal-intensity doublets. Therefore, as shown in Fig. 3(C), the ^{13}C NMR spectrum of CTA II is characterized simply as an overlap of the ^{13}C subspectra of the two kinds of glucopyranose residues.

According to the structure of CTA II proposed on the basis of fiber X-ray diffraction analysis [3], the unit cell of this allomorph is considered to be orthorombic with space group $P2_12_12_1$ and dimensions $a = 24.68$ Å, $b = 11.52$ Å, $c = 10.54$ Å. The unit cell has 4 chains, 2 parallel and 2 antiparallel. The 2 chains in each parallel and antiparallel pairs are related via 2_1 screw axes positioned outside of the chains. In the suggested structure, all glucopyranose residues in the unit cell of CTA II have an identical conformation. In this experiment, on the other hand, it was revealed that ring carbons except for C1 experienced magnetic inequivalence and appeared as doublets in the CP/MAS ^{13}C NMR spectra of CTA II (Figs. 3(C) and 5).

With respect to the C4–C5–C6–O6 dihedral angle of the CTAs, we previously suggested that CTA I and CTA II are distinguished by the conformational difference around the exocyclic C5–C6 bonds on the basis of the three C6 chemical shifts in both allomorphs [17]. On the other hand, the results of the conformational energy calculations [3,33] for CTA indicated that the difference of the C6 chemical shifts in CTA could not explained by the changes in the C4–C5–C6–O6 dihedral since the *gauche–gauche* conformation of the C4–C5–C6–O6 dihedral angle of CTA was severely restricted by the acetyl groups. In relation to the conformation for the exocyclic C5–C6 bond, Horii et al. [34] reported that chemical shifts of C6 of carbohydrates fall into three groups of 62, 64, and 66 ppm, which are related to *gauche–gauche*, *gauche–trans*, and *trans–gauche* conformations, respectively. In the CP/MAS ^{13}C NMR spectra of CTA I and CTA II, the chemical shifts of C6 differ strongly. The C6 signal of CTA I appears at 62.5 ppm, while C6 doublet of CTA II are observed at 67.3 and 65.2 ppm. Since the C6 signal of cellulose is shifted downfield by the acetylation of hydroxyl groups [24], the correspondence between chemical shift and conformation proposed by Horii et al. [34] may not be directly applicable. However, the ^{13}C chemical shift differences observed in this study are large enough to indicate a conformational difference in the exocyclic C5–C6 bonds between CTA I and CTA II.

Beside backbone structure of CTA II, VanderHart et al. [14] suggested that there are different conformations of methyl groups bound to C6 of CTA II and that the methyl resonance at 23 ppm in the CTA II spectrum may be associated with the acetate group at one of these C6 sites, on the basis of the chemical shifts of the methyl carbons. In the $^{1}H-^{13}C$ correlation spectrum of CTA II, the ^{1}H chemical shifts of protons attached to methyl carbons whose resonances appear at 21–19 ppm ranged between 1.1 and 0.6 ppm, while the ^{1}H shifts of the methyl group whose carbon resonance appears at 23 ppm is shifted downfield at 1.7 ppm. The notable difference in the ^{1}H shifts of the methyl groups of CTA II strongly suggested the conformational difference in the methyl groups of CTA II. In addition, the large downfield shifts of protons attached to the methyl carbon at 23 ppm were enough to suggest that the conformation of the methyl group at one of the C6 sites would differ with those of the other methyl groups if the ^{13}C resonance that appears at 23 ppm could be assigned to the methyl group at one of the C6 sites in CTA II.

CTA I is a unique allomorph in the series of cellulose and CTA allomorphs, since each carbon nucleus shows only a single resonance, in contrast with the ^{13}C spectra of other allomorphs, where most carbons display multiple resonances [14,35,36]. This suggested that the asymmetric unit of CTA I is one glucopyranose residue; this was strongly supported by the new finding that the number of ^{1}H resonances of protons attached to ring carbons in CTA I agrees with the number of protons in the glucopyranose residue, except for the acetyl groups. This deduction contradicts the proposed structure of CTA I [2] as having two independent chains per unit cell with a $P2_1$ space group. If the proposed structure were correct, there should be two magnetically non-equivalent sites in the unit cell of CTA I. This is not supported by our NMR data. In the relationship between the structure and the ^{13}C spectrum of CTA I, the new structural model of cellulose III_I, which was recently proposed by Wada et al. [37,38] on the basis of the results of X-ray and synchrotron diffractions of this allomorph, is interesting. The previous structure model of cellulose III_I [39] had been considered to have a $P2_1$ space group with two independent cellulose chains per unit cell, which is very close to the proposed structure of CTA I [2]. The previous model of cellulose III_I indicates that there should be two independent glucopyranose moieties in the crystal, which conflicts with the fact that each carbon nucleus appears as a singlet in the CP/MAS ^{13}C spectrum of this allomorph [35,36,40–42]. On the other hand, the refined model proposed by Wada et al. [38] is described with a one-chain unit cell and a $P2_1$ space group, with the cellulose chain axis on one of the 2_1 screw axes of the cells. In the

new cell of cellulose III_I, one glucopyranose residue becomes the asymmetric unit, which agrees well with the fact that the CP/MAS ^{13}C spectrum of cellulose III_I presented only six resonance peaks. In the case of CTA I, therefore, it is considered that only one glucopyranose moiety should be an asymmetric unit in the crystal structure, since all protons as well as glucopyranose residue in the CTA I appear as respective singlets.

The suggestion that the symmetric unit of CTA I is in fact one glucopyranose residue can be strongly supported by the number of ^{1}H and ^{13}C resonances for the methyl group of this allomorph. In the MAS-J-HMQC spectrum of CTA II, the methyl carbon resonances at 22.7 and 20.3 ppm provides complex $^{1}H-^{13}C$ cross-peaks. The lowfield ^{13}C signal at 22.7 ppm gives one cross-peak in the ^{1}H chemical shifts of 1.7 ppm, while the highfield one at 20.3 ppm provides multiplet. In addition, at least three cross-peaks could be detected in the multiplet patterns. These findings indicate that the structure of CTA II has at least two kinds of glucopyranose moieties in the unit cell. In contrast to the complex $^{1}H-^{13}C$ correlation patterns for the methyl groups of CTA II, a doublet for the methyl carbon resonances of CTA I provide respective one cross-peak in the MAS-J-HMQC spectrum of this allomorph. By estimating the position of the two cross-peaks in the ^{1}H direction, all protons of methyl groups could be assigned as 0.7 ppm. This strongly suggests that the methyl groups of the respective carbon sites are in the same conformation, which conflicts with the structure of CTA I proposed by the X-ray analysis of the fibrous CTA I [2]. It is therefore, necessary to refine the CTA I structure by applying diffraction techniques with high resolution.

Very recently, Sternberg et al. [43] performed crystal structure refinements of cellulose I_α, I_β, and II by means of force field optimization with ^{13}C chemical shift data of these crystalline allomorphs. To the best of our knowledge, this is the first crystal structure refinement of cellulose performed using solid-state ^{13}C chemical shifts, and the force field methods [43,44] in combination with ^{13}C chemical shifts in solid-state is expected to become a valuable technique for elucidation of the crystal structure of biopolymers such as cellulose and cellulose derivatives. Such a technique in combination with the ^{1}H as well as the ^{13}C chemical shifts data of CTA polymorphs provided herein may lead to determination of the correct structure of CTA I and CTA II.

4. Conclusions

In conclusion, ^{1}H and ^{13}C chemical shifts of the two crystalline allomorphs of CTA were completely assigned by the through-bond $^{1}H-^{13}C$ and $^{13}C-^{13}C$, respectively, correlation experiments in the solid state. The 2D $^{13}C-^{13}C$ correlation spectrum of CTA II revealed that the CP/MAS ^{13}C NMR spectrum of crystalline CTA II was attributed to the overlap on the ^{13}C subspectra of two kinds of glucopyranose residues, in contrast with the ^{13}C spectrum of CTA I, where each carbon displays only a single resonance. The respective numbers of ^{13}C and ^{1}H shifts of CTA I agreed with those of the glucopyranose moiety in the allomorph, indicating that the asymmetric unit of CTA I is only one glucopyranose residue. This deduction disagrees with the structure of CTA I [2] proposed by X-ray analysis, in which each unit cell has two independent chains. In addition, conformational differences in the exocyclic C5–C6 bonds between CTA I and CTA II were strongly suggested by the notable difference in the ^{1}H as well as ^{13}C chemical shifts at the C6 sites of these allomorphs.

References

[1] Sprague BS, Riley JL, Noether HD. Text Res J 1958;28:275–87.
[2] Stipanovic AJ, Sarko A. Polymer 1978;19:3–8.
[3] Roche E, Chanzy H, Boudeulle M, Marchessault RH, Sundararajan P. Macromolecules 1978;11:86–94.
[4] Dulmage WJJ. Polym Sci 1957;26:277–88.
[5] Gardner KH, Blackwell J. Biopolymers 1974;13:1975–2001.
[6] French AD. Carbohydr Res 1978;61:67–80.
[7] Woodcock C, Sarko A. Macromolecules 1980;13:1183–7.
[8] Kolpak KJ, Blackwell J. Macromolecules 1976;9:273–8.
[9] Stipanovic AJ, Sarko A. Macromolecules 1976;9:851–7.
[10] Helbert W, Sugiyama J. Cellulose 1998;5:113–22.
[11] Watanabe S, Takai M, Hayashi J. J Polym Sci, Part C 1968;23:825–35.
[12] Takai M, Fukuda K, Hayashi J. J Polym Sci, Polym Lett Ed 1987;25:121–6.
[13] Creely JJ, Conrad CM. Text Res J 1965;35:184–7.
[14] VanderHart DL, Hyatt JA, Atalla RH, Tirumalai VC. Macromolecules 1996;29:730–9.
[15] Kono H, Numata Y, Nagai N, Erata T, Takai M. J Polym Sci, Part A: Polym Chem 1999;37:4100–7.
[16] Horii F, Yamamoto H, Kitamaru R, Tanahashi M, Higuchi T. Macromolecules 1987;20:2946–51.
[17] Kono H, Erata T, Takai M. J Am Chem Soc 2002;124:7512–8.
[18] Lesage A, Bardet M, Emsley L. J Am Chem Soc 1999;121:10987–93.
[19] Lesage A, Sakellariou D, Steuernagel S, Emsley L. J Am Chem Soc 1998;120:13194–201.
[20] Lesage A, Emsley L. J Magn Reson 2001;148:449–54.
[21] Hestrin S, Schramm M. Biochem J 1954;58:345–52.
[22] Kono H, Yunoki S, Shikano T, Fujiwara M, Erata T, Takai M. J Am Chem Soc 2002;124:7506–11.
[23] Tanghe LJ, Genung LJ, Mench JW. Methods Carbohydr Chem 1963;3:193–212.
[24] Buchanan CM, Hyatt JA, Kelly SS, Little JL. Macromolecules 1990;23:3747–55.
[25] Nevell TP, Zeronian SH. Polymer 1962;3:187–94.
[26] Metz G, Wu X, Smith SO. J Magn Reson A 1994;110:219–27.
[27] Bennett AE, Rienstra CM, Auger M, Lakshmi KV, Griffin RG. J Chem Phys 1995;103:6951–8.
[28] Marion D, Wüthrich K. Biochem Biophys Res Commun 1983;113:967–74.
[29] Lee M, Goldberg WI. Phys Rev 1965;140A:1261–71.
[30] Bielecki A, Kolbert AC, Levitt MH. Chem Phys Lett 1989;155:341–6.
[31] States DJ, Haberkorn RA, Ruben DJ. J Magn Reson 1982;48:286–92.
[32] Kono H, Erata T, Takai M. Macromolecules 2003;36:5131–8.
[33] Wolf RM, Francotte E, Glasser L, Simon I, Scheraga HA. Macromolecules 1992;25:709–20.

[34] Horii F, Hirai A, Kitamaru R. Polym Bull 1983;10:357–61.
[35] Isogai A, Usuda M, Kato T, Uryu T, Atalla RH. Macromolecules 1989;22:3168–72.
[36] Kono H, Erata T, Takai M. Macromolecules 2003;36:3589–92.
[37] Wada M. Macromolecules 2001;34:3271–5.
[38] Wada M, Heux L, Isogai A, Nishiyama Y, Chanzy H, Sugiyama J. Macromolecules 2001;34:1237–43.
[39] Sarko A, Southwick J, Hayashi J. Macromolecules 1976;9:857–63.
[40] Fyfe CA, Dudley RL, Stephenson PJ, Deslandes Y, Hamer GK, Marchessault RH. J Macromol Sci Rev Macromol Chem Phys 1983; C23:187–216.
[41] Chanzy H, Henrissat B, Vincendon M, Tanner SF, Belton PS. Carbohydr Res 1987;160:1–11.
[42] Hayashi J, Kon H, Takai M, Hatano M, Nozawa T. The crystal structures of cellulose. ACS symposium series 340. Washington DC: American Chemical Society; 1987. p. 135–50.
[43] Sternberg U, Koch FTh, Prieß W, Witter R. Cellulose 2003;10:189–99.
[44] Witter R, Prieß W, Sternberg U. J Comput Chem 2002;23:298–305.